

Vibration control of a time-varying modal-parameter footbridge: study of semi-active implementable strategies

José M. Soria^a, Iván M. Díaz^{*} and Jaime H. García-Palacios^b

Department of Continuous Medium Mechanics and Theory of Structures, ETS Ingenieros de Caminos,
Universidad Politécnica de Madrid, ES 28040, Madrid, Spain

(Received March 7, 2017, Revised May 8, 2017, Accepted September 3, 2017)

Abstract. This paper explores different vibration control strategies for the cancellation of human-induced vibration on a structure with time-varying modal parameters. The main motivation of this study is a lively urban stress-ribbon footbridge (Pedro Gómez Bosque, Valladolid, Spain) that, after a whole-year monitoring, several natural frequencies within the band of interest (normal paring frequency range) have been tracked. The most perceptible vibration mode of the structure at approximately 1.8 Hz changes up to 20%. In order to find a solution for this real case, this paper takes the annual modal parameter estimates (approx. 14000 estimations) of this mode and designs three control strategies: a) a tuned mass damper (TMD) tuned to the most-repeated modal properties of the aforementioned mode, b) two semi-active TMD strategies, one with an on-off control law for the TMD damping, and other with frequency and damping tuned by updating the damper force. All strategies have been carefully compared considering two structure models: a) only the aforementioned mode and b) all the other tracked modes. The results have been compared considering human-induced vibrations and have helped the authors on making a decision of the most advisable strategy to be practically implemented.

Keywords: semi-active vibration control; dynamic behavior; time-varying modal-parameters; human-induced vibration; footbridge

1. Introduction

The current trend towards lighter and slender structures is resulting in structures with less inherent damping and lower natural frequencies (Gunaydin *et al.* 2015, Casciati and Casciati 2016), which are more susceptible to be excited by human users. Examples of notable vibrations under human-induced excitation have been reported in footbridges, office buildings, shopping malls and sport stadia, amongst other structures, mainly affecting their serviceability (Moutinho *et al.* 2015).

Within the possible solutions to overcome vibration serviceability problems in footbridges, the inclusion of damping devices to the structure seems to be the easiest way to improving the vibration performance. Among passive control devices available for implementation, Tuned Mass Damper (TMD) based strategies are usually adopted for footbridges (Caetano *et al.* 2010, Moutinho *et al.* 2010, Casado *et al.* 2013, Bortoluzzi *et al.* 2015). Passive control strategies are easy to design and do not require external power. However, they have relatively poor performance for low-level vibration and they might exhibit a lack of

performance due to the off-tuning issue. Both are well-known problems shown by TMDs when the have to cope with: 1) low-amplitude human-induced vibrations (as those usually happen in pedestrian structures), 2) vibration modes with time-varying modal parameters, and 3) vibration response coming from other modes different from the targeted mode. Under these circumstances, passive mass dampers may be upgraded to semi-active or fully-active mass dampers.

In the last decades, semi-active control systems have been studied intensively (Jung *et al.* 2004, Casciati *et al.* 2006, Nagarajaiah and Jung 2014) since they combine the best features of both passive (stability, robustness) and active (adaptability) control systems using low power consumption to operate (as compared to fully-active systems). However, they still need a feedback control scheme as active systems (Pereira *et al.* 2014, Casciati and Casciati 2016). Semi-active control for building under seismic actions has been intensively studied (Chang *et al.* 2013, Askari *et al.* 2016). However, application of semi-active control strategies for human-induced vibration are rarely formed. Regarding footbridge, the control law may continuously change the TMD parameters (Weber 2013) or may be based on ON/OFF control strategies (Moutinho 2015). The latter option, which might be not as effective as the former, is easier for practical implementation and maintenance.

An in-service steel-plated stress-ribbon footbridge is considered in this work. This structure was previously analyzed in Soria *et al.* (2016). The influence of the environmental factors on modal parameter estimation was

*Corresponding author, Dr.
E-mail: ivan.munoz@upm.es

^a Ph.D.
E-mail: jm.soria@upm.es

^b Professor
E-mail: jaime.garcia.palacios@upm.es



(a) Landscape view



(b) Distribution of sensors

Fig. 1 Pedro Gómez Bosque footbridge (images courtesy of J. Muñoz-Rojas)

therefore extensively studied. It was found that this structure has the most perceptible vibration mode at approximately 1.8 Hz (within the normal range of walking).

Through a peered analysis of a full-year monitoring, it was obtained that this mode changes up to 20% during the year with both seasonal and daily trends and that these changes were mainly explained by temperature variation. Furthermore, the structure has other vibration modes with natural frequencies smaller than 4 Hz that might also be excited by human-induced vibrations. Thus, this paper studies the performance of two semi-active TMD (STMD) strategies as compared to a classical TMD for this structure. Considering firstly, only the aforementioned mode (single degree of freedom, SDOF, model) and secondly, all the modes with natural frequencies smaller than 4 Hz (multi-degree of freedom, MDOF, model), over time. The two STMDs are considered to be implemented using magnetorheological (MR) damper and the control laws are implementable in practice.

The paper continues with the structure description, its monitoring system and the considered structure models. Section 3 describes the vibration control strategies. Section 4 discusses about the results and, finally, some conclusions are drawn.

2. The stress-ribbon bridge

2.1 Structure description and its monitoring

Pedro Gómez Bosque Footbridge, sited in Valladolid (Spain), is a slender and lightweight structure that creates a pedestrian link over the Pisuerga River between a sport complex and the city centre (see Fig. 1). This bridge, built in 2011, is a singular stress-ribbon footbridge of 85 m span born by a pre-tensioned catenary-shape steel band (of only 30 mm thick) and precast concrete slabs lying on the band (Narros 2011).

A structural vibration monitoring system was devised in order to continuously estimate the modal parameters of the structure and to assess their changes under varying environmental conditions. Therefore, in addition to the accelerometers needed to perform a modal analysis, sensors for the wind and environmental temperature conditions were installed. The monitoring system comprises 18 triaxial accelerometers, 9 at each side of the deck, a temperature sensor and an anemometer with a vane (see Fig. 1). Wires and acceleration sensors were installed inside the handrail so the structure aesthetic was not modified in any way. The monitoring system is explained in detail in references Sebastián *et al.* (2013) and Soria *et al.* (2016). The novelty of this system is that low-cost MEMS accelerometers properly conditioned were used resulting finally in a really cheap monitoring system.

2.2 Tracking of vibration modes

The natural frequency estimates for the more lingering modes over 1-year of continuous dynamic monitoring were

Table 1 Summary of identified natural frequencies and damping ratios for one year monitoring and their statistics: mean frequency (\bar{f}), mean damping ($\bar{\zeta}$), standard deviation (Std) and corresponding variation (ν)

Mode	Frequency			Damping			Repeatability
	\bar{f} (Hz)	Std	ν (%)	$\bar{\zeta}$ (%)	Std	ν (%)	
1	1.0482	0.0152	14.23	0.3665	0.1710	147.89	9667 (44.7%)
2	1.4145	0.0107	35.26	0.3381	0.1513	110.74	10619 (49.1%)
3	1.5440	0.0181	27.63	0.6498	0.2357	133.62	9886 (45.7%)
4	1.7937	0.0291	20.27	0.4192	0.1502	221.88	13817 (63.8%)
5	1.8594	0.0168	6.87	0.5718	0.1605	234.74	9936 (45.9%)
6	2.3117	0.0425	15.01	0.3753	0.1474	128.54	8746 (40.4%)
7	3.3821	0.0549	42.95	0.3868	0.1191	103.96	12210 (56.4%)
8	3.5512	0.0524	51.87	0.7226	0.1884	157.48	9237 (42.7%)
9	3.9610	0.0624	8.95	0.3853	0.1185	230.82	10183 (57.8%)

derived in Soria *et al.* (2016). Up to nine vibration modes below 4 Hz were tracked. Fig. 2 shows the tracked frequency estimates, in which some occasional stops due to technical problems are observed. The covariance-driven Stochastic Subspace Identification method was used for the operational modal analysis estimation (Peeters and De Roeck 1999). Table 1 shows the following statistics of the estimation: mean, standard deviation, absolute percentage variation and their repeatability (the percentage of estimation for which a particular mode was successfully estimated). Note that the fourth mode at 1.79 Hz (with a damping ratio of only 0.42%) corresponds to the highest repeatability. Fig. 3 shows the first six modal shapes of identified vibration modes of Table 1.

2.3 Structure models

The fourth mode of Table 1 was shown to be the most critical one for the vibration serviceability assessment. Fig. 4 shows the distribution of the natural frequency and damping ratio estimates of mode 4 for the full year. As it can be observed, the damping estimates fit to a normal distribution whereas the frequency estimates do not fit to it. Besides, the average value and the most repeated one are clearly different for frequency estimates.

 Table 2 Summary of modal participation factors, α_i , for each vibration mode at the maximum amplitude node of mode 4

Mode	\bar{f} (Hz)	α (kg^{-1})
1	1.0482	$3.26 \cdot 10^{-6}$
2	1.4145	$1.30 \cdot 10^{-5}$
3	1.5440	$1.13 \cdot 10^{-5}$
4	1.7937	$2.00 \cdot 10^{-5}$
5	1.8594	$1.32 \cdot 10^{-5}$
6	2.3117	$1.19 \cdot 10^{-5}$
7	3.3821	$5.11 \cdot 10^{-6}$
8	3.5512	$2.10 \cdot 10^{-5}$
9	3.9610	$2.51 \cdot 10^{-6}$

Two structure models are considered to study the performance of the control strategies. Firstly, a SDOF model corresponding to mode 4 is considered (Table 1). It is assumed that the control device is placed at the point of maximum displacement of mode 4 (at one lateral side of the deck at 77.25 m from abutment). Secondly, the effect of other modes at that point is included in such a way that a MDOF system is considered. The frequency and damping for each vibration model will change according to estimates over the year. Table 2 shows the modal participation factors, α_i , at such location which will be considered fixed values and have been obtained from an updated finite element mode (Castaño *et al.* 2015).

As usual, the Transfer Function between the structure acceleration and the applied force in the Laplace domain is as follows

$$G(s) = \sum_{i=1}^N \frac{\alpha_i s^2}{s^2 + 2\zeta_i \omega_i s + \omega_i^2}, \quad (1.1)$$

in which $s = j\omega$, $\omega = 2\pi f$ being the circular frequency (rad/s) and f the natural frequency (Hz), α_i modal participation factor (taken from Table 2), ω_i is the circular frequency and ζ_i is the damping ratio. The values of these varying modal parameters are those estimated experimentally for the full-year (in the footbridge and represented by their mean value in Table 1). N is the number of vibration modes taken into account in the model ($N=1$ and $N=9$ for the SDOF and MDOF models, respectively).

Figure 5a shows the 13817 models considered the case of SDOF system. Fig. 5(b) shows the 1721 models considered for the case of MDOF system. This is the number of estimations for which the ninth first modes are estimated simultaneously.

$$F(t) = F_0(f) \cdot \sin(\psi(t)), \quad (1.2)$$

in which $\psi(t) = 2\pi f(t)t$ is the phase of the chirp signal, t being the time, which is defined depending of the instantaneous frequency

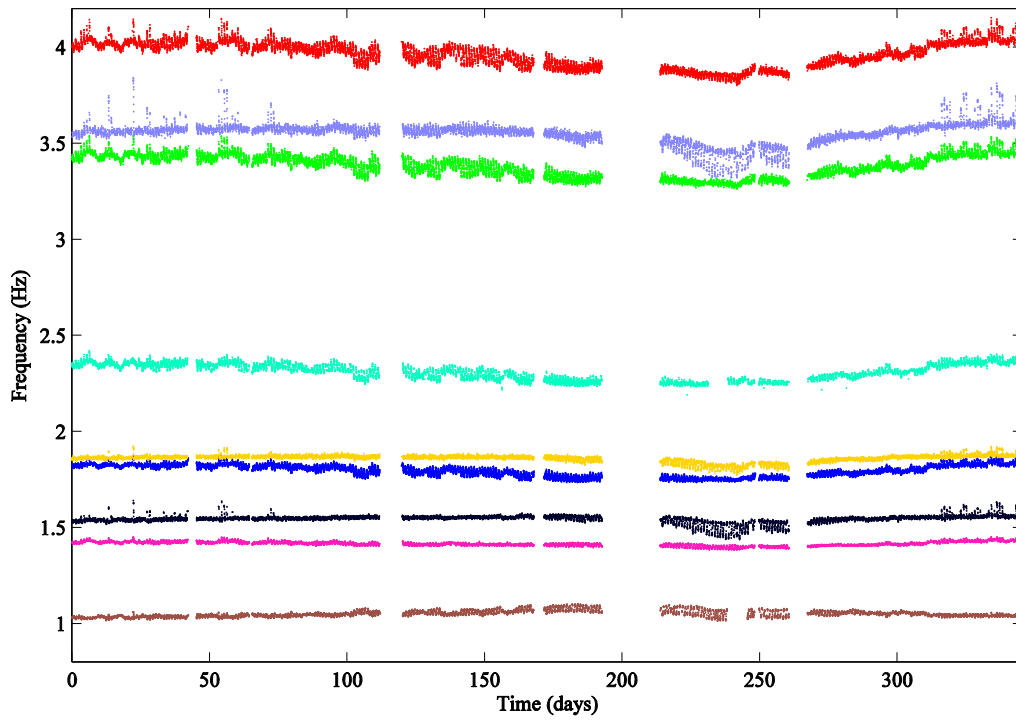


Fig. 2 Tracked frequency estimates for the full year

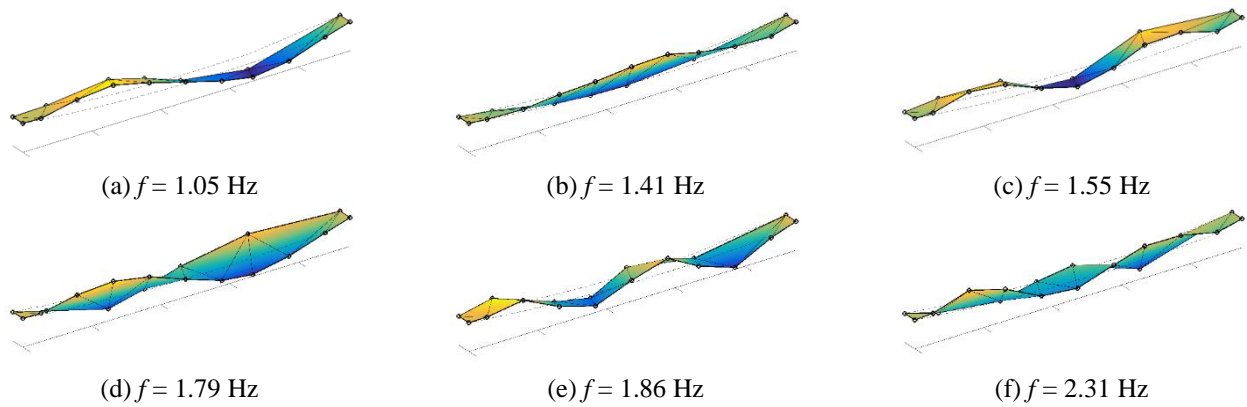


Fig. 3 First six modal shapes for vibration modes of Table 1

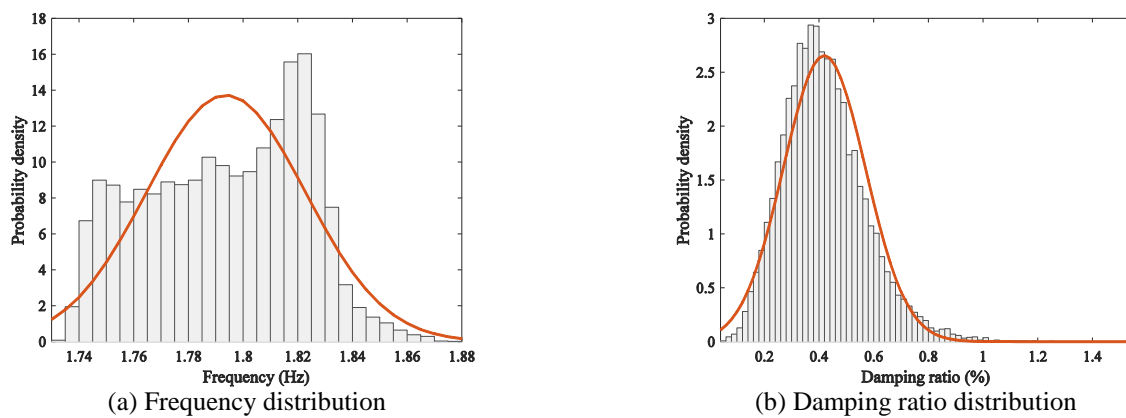


Fig. 4 Distribution density. The line shows the normal distribution with the same mean and standard deviation as the original distribution density

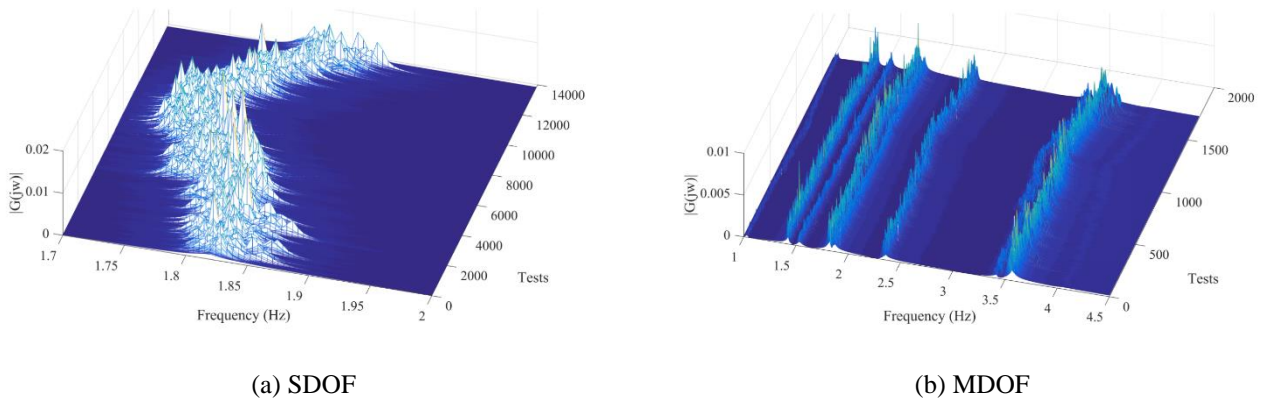
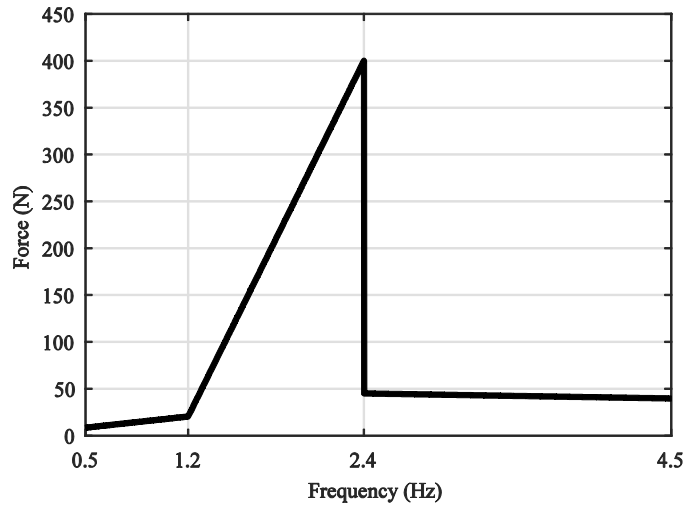


Fig. 5 Magnitude of Transfer Functions of the models considered over the year


 Fig. 6 Weighted force amplitude, $F_0(f)$

$$\begin{aligned} f(t) &= f_i + kt, \\ k &= \frac{f_f - f_i}{T_f}, \end{aligned} \quad (1.3)$$

$$\begin{aligned} f(t) &= f_i + kt, \\ k &= \frac{f_f - f_i}{T_f}, \end{aligned} \quad (1.4)$$

where k is the rate of frequency change, f_f is the final frequency, f_i is the starting frequency and T_f is the time it takes to sweep from f_i to f_f . The frequency range has been chosen in order to excite the nine vibration modes below 4 Hz. The final time, T_f , has been 500s and 1000s, for the SDOF and MDOF system, respectively. These values were chosen to ensure that sweeping at each frequency is sufficiently slow so that the results do not depend on the final time.

The amplitude of the force has been frequency weighted according to dynamic load factors for walking induced vertical forces (Brownjohn *et al.* 2004, Wang *et al.* 2016).

The following definition for $F_0(f)$ has been taken here

Fig. 6 shows $F_0(f)$ for the considered frequency range. Note that the amplitude is representative of the load imparted by a pedestrian walking at different frequencies. Besides, this input force can be easily generated by a shaker to assess control devices designed for canceling human-induced vibration.

3.2 Passive control: Tuned mass damper

A TMD consists of a secondary mass (also called moving or inertial mass) attached to the structure by means of springs and dampers. The TMD mass is fixed as a fraction of the modal mass (which is the inverse of the modal participation factor α_i , Eq. (1)) of the targeted vibration mode; the stiffness of the springs is selected to

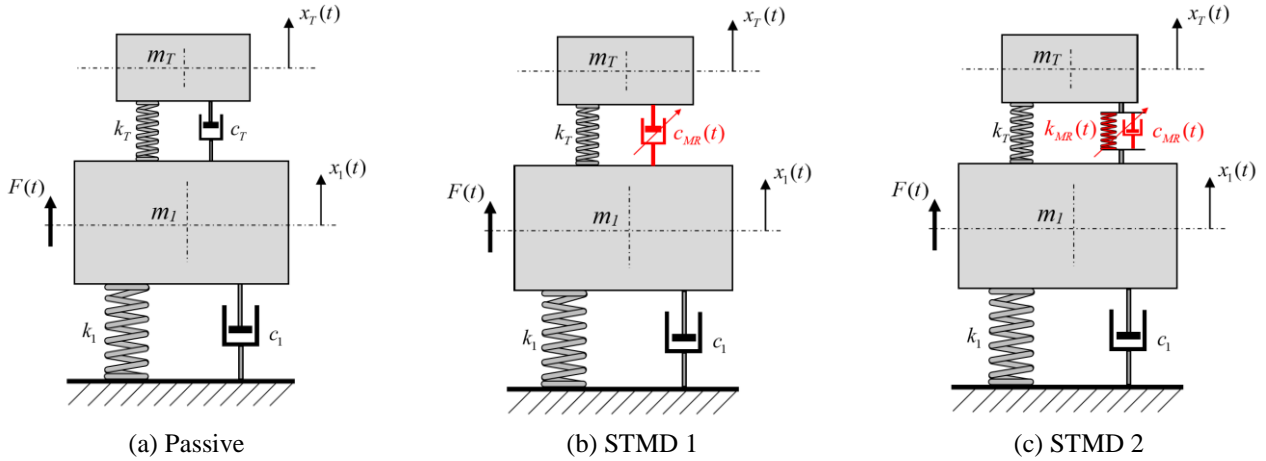


Fig. 7 Model of the devices installed on a primary structure. Red symbol (\uparrow) means changing over time

obtain the optimum TMD frequency, and the viscous dampers ensure the operation of the TMD in a range of frequencies around the tuning frequency.

Fig. 7(a) shows the model of a classical TMD composed of an inertial mass m_T attached to a primary system by means of a spring of constant k_T and a viscous damper of constant c_T . The primary system is the structure modeled as a SDOF system, which is composed of a mass m_1 , a spring constant k_1 and a viscous damper of constant c_1 .

These physical parameters are equivalent to the modal parameters of Eq. (1) with $N=1$: $\alpha_1=1/m_1$, $k_1=\omega_1^2/\alpha_1$ and $c_1=(2\zeta_1\omega_1)/\alpha_1$.

The TMD has been designed using the Den Hartog (1985) formulas and only mode 4 is considered for TMD design ($i=1$ in Eq. (1)). It is well known and widely used in real structures for the mitigation of resonance vibration problems and it is chosen in this study as a benchmark damper, as it is also done in Weber (2013), for instance.

The TMD properties are

$$m_T = \mu m_1, \quad (1.5)$$

$$\eta = \frac{1}{1 + \mu}, \quad (1.6)$$

$$\zeta_T = \sqrt{\frac{3\mu}{8(1 + \mu)^3}}, \quad (1.7)$$

in which $\mu = m_T / m_1$ is the mass ratio, which is assumed to be 1% ($m_T=500$ kg), $\eta = \omega_T / \omega_1$ is the frequency ratio and the stiffness and damping ratio for the TMD are obtained from

$$k_T = \omega_T^2 m_T, \quad (1.8)$$

$$c_T = 2\zeta_T m_T \omega_T, \quad (1.9)$$

respectively.

3.3 Semi-active control 1

Fig. 7(b) shows a STMD (hereafter denoted as STMD 1) in which the TMD damper is supposed to be a MR-damper ($c_{MR}(t)$), whose damping can be changed continuously. A phase control strategy for the TMD damping is considered here. More concretely, the adapted version from Chung *et al.* (2013) proposed by Moutinho (2015) has been adopted since this is clearly geared to practical implementation due to the quantities employed: the structure acceleration instead of displacement and the TMD mass velocity instead of the relative velocity, as usual (Koo *et al.* 2004). The control law achieves a phase lag between the control force (the force coming from the TMD) and structure displacement close to 90° even in situation of significant detuning. The control law adopted is of ON/OFF type due to its simplicity. Thus, the adopted control law is defined as follows (Moutinho 2015):

$$\begin{cases} \ddot{x}_1 \cdot \dot{x}_T \leq 0 & \Leftrightarrow & c_{MR} = c_{\min} \quad (\text{normal functioning}) \\ \ddot{x}_1 \cdot \dot{x}_T > 0 & \Leftrightarrow & c_{MR} = c_{\max} \quad (\text{blocking functioning}) \end{cases}, \quad (1.10)$$

in which $c_{\max} = 50 \cdot c_{\min}$, c_{\min} is the optimal damping obtained from Eq. (9), \ddot{x}_1 is the structure acceleration (obtain by an accelerometer) and \dot{x}_T is the absolute velocity of the TMD mass (which might be obtained from the integration of an accelerometer signal installed on the TMD mass).

3.4 Semi-active control 2

Fig. 7(c) depicts the STMD strategy proposed by Weber (2013) and denoted as STMD 2 hereafter. The key feature of this control law is that the energy dissipation and natural frequency of the STMD, respectively, are adjusted according to Den Hartog's formula in real time to f_w instead of f_1 , f_w being the actual instantaneous frequency of the vibration response, independently if this frequency corresponds to the resonant frequency of the targeted vibration mode or represents an excitation

frequency due to forced excitation out of resonance. The MR damper works in parallel with a passive spring designed according to Den Hartog's formula (see Figure 7c), denoted by k_T .

The MR damper emulates the sum of a controllable stiffness force (positive or negative), F_k , and a controllable dissipative force, F_c , as follows

$$F = F_k + F_c, \quad (1.11)$$

These forces are clipped to zero, which yields to the semi-active force, F_{MR} , as follow

$$F_{MR} = \begin{cases} F, & \text{sgn}(\dot{x}_1 - \dot{x}_T) \cdot F \\ 0, & \text{sgn}(\dot{x}_1 - \dot{x}_T) \cdot F' \end{cases}, \quad (1.12)$$

in which $\text{sgn}(\dot{x}_1 - \dot{x}_T)$ is the sign of the relative velocity between the structure and TMD mass.

The actual frequency, f_w , is estimated from the zero-crossing of the relative displacement, $x_s - x_T$, through the half period time, T_{half} . The actual frequency is then estimated as follows

$$f_w = \frac{1}{2T_{\text{half}}}. \quad (1.13)$$

Thus, the stiffness and energy dissipation of the STMD 2 are tuned to the actual frequency of vibration f_w by the modified mass ratio $\tilde{\mu}$ that depends on the frequency shift between f_w and f_1 as follows

$$\tilde{\mu} = \mu \left(\frac{f_w}{f_1} \right), \quad (1.14)$$

And then, the damper properties are derived as

$$k_{MR} = k_1 \frac{\tilde{\mu}}{(1 + \tilde{\mu})^2} - k_T, \quad (1.15)$$

$$\zeta_{MR} = \sqrt{\frac{3\tilde{\mu}}{8(1 + \tilde{\mu})^3}}, \quad (1.16)$$

$$c_{MR} = 2\zeta_{MR}m_T(2\pi f_w). \quad (1.17)$$

Finally, the control forces to compute (11) and apply the semi-active control law (12) are

$$F_k = k_{MR}(x_1 - x_T), \quad (1.18)$$

$$F_c = \text{sgn}(\dot{x}_1 - \dot{x}_T) \left\{ \frac{\pi}{4} c_{MR} (2\pi f_w) (x_1 - x_T) \right\}. \quad (1.19)$$

The reader can consult the article of Weber (2013) to go deeper into the algorithm. It should be mentioned that this algorithm requires measuring the relative displacement as well as knowing the sign of relative velocity. This might be

undertaken using a displacement transducer between the structure and TMD mass. It is worth mentioning that the implementation of the control law of STMD 2 is more complicated than the implementation of the one of STMD 1.

4. Results

Four cases are analyzed (see section 2.3), SDOF and MDOF systems for nominal and full year analysis:

- SDOF systems

- Nominal case

A SDOF model of the structure with mean frequency and mean damping (see Fig. 4) of the full year is adopted.

- Full year case

13817 SDOF models estimated for the full year are simulated. Fig. 5(a) illustrates the models. Control strategy degradation from nominal case is studied in this case.

- MDOF

- Nominal case

A MDOF model with the ninth first vibration modes is considered. Mean values for frequency and damping (see Fig. 2) are used for the nominal model. The influence of additional modes on the control performance is studied against SDOF nominal case.

- Full year case

A value of 1712 MDOF models are obtained making the intersection between the modal estimates of the 9 tracked vibration modes over the full year monitoring. The effects of additional time-varying modes is studied. Fig. 5(b) illustrates the model variations over time.

The loading force described in 3.1 is applied to the structural model for the uncontrolled case and for the three control strategies described previously. The control performance of these three strategies are compared in time and frequency domain:

- In time domain, the Maximum Transient Vibration Value (MTVV) calculated from the 1s running root-mean square acceleration is considered (ISO 10137:2007). The MTVV is adopted for current standards as vibration predictor for the serviceability assessment.
- In frequency domain, the H_∞ and H_2 norms represent scalar values of control performance (Weber *et al.* 2006).

The vibration reduction for each case is computed as follows. For nominal cases, the vibration reduction is directly obtained as (uncontrolled value – controlled value)/uncontrolled value. For the full year cases, the Cumulative Distribution Function (CDF) curves are computed. Thus, the vibration reduction is obtained from the total area between the CDF curve and y-axis. That is, the solution is computed as (uncontrolled CDF_{area} – controlled CDF_{area})/uncontrolled CDF_{area}. Through this procedure, a single value can be derived to quantify the reduction performance for full year analysis.

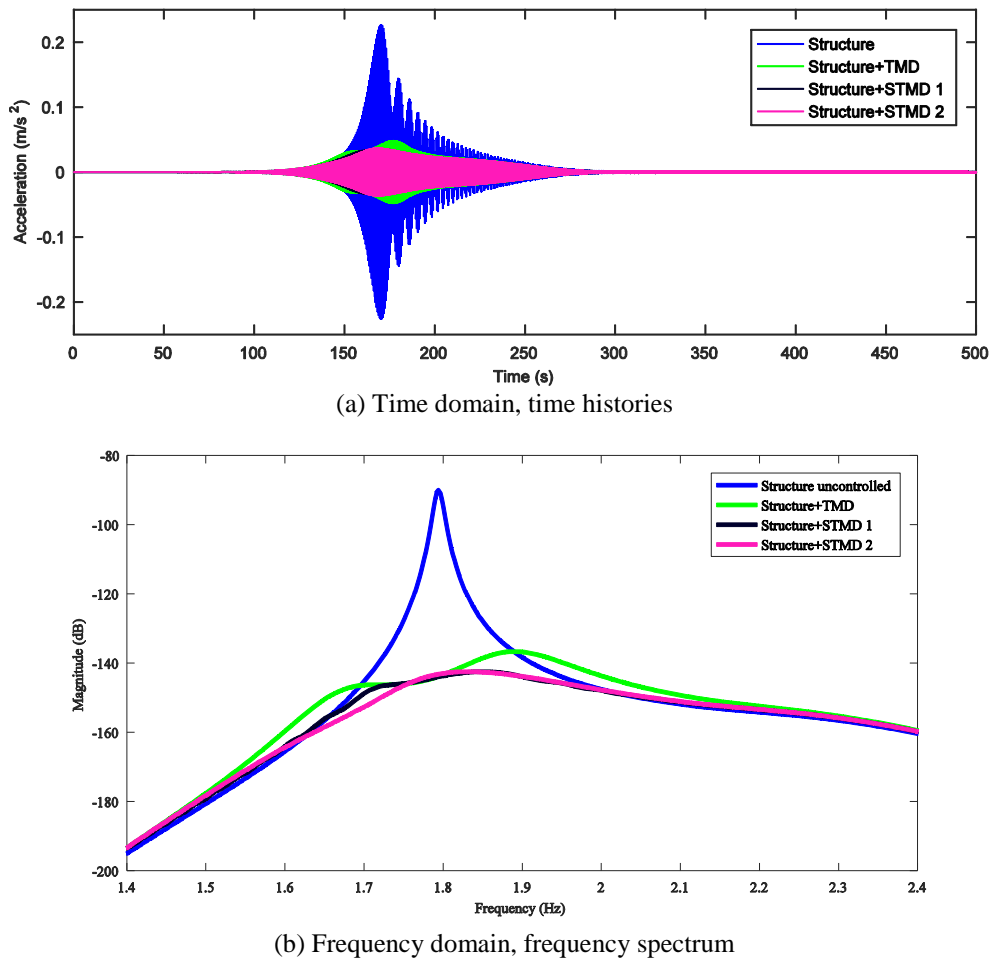


Fig. 8 Response of SDOF system

4.1 Single degree of freedom system

4.1.1 Nominal case

Fig. 8 shows the acceleration responses and their corresponding frequency spectra. It is observed that both STMDs, 1 and 2, improve marginally the results as compared to the TMD. The vibration reductions for each case are 79.04%, 84.08% and 83.78% (MTVV), 90.23%, 92.69% and 92.69% (H_∞) and 34.57%, 42.28% and 42.75% (H_2) for TMD, STMD 1 and STMD 2, respectively.

4.1.2 Full year tests

The TMD might detune when variations into the modal parameters of the structure take place, as it is the case studied here. In this case, the most-repeated modal properties (frequency and damping ratio) are 1.82 Hz and 0.37%, respectively (see Fig. 4). Then, these values have been adopted to tune the control device. Fig. 9 shows the MTVV obtained for the uncontrolled case and the three control strategies (TMD, STMD 1 and STMD 2).

Fig. 10 shows CDF curves for MTVV, H_∞ and H_2 obtained for the full year distribution response. It is worth

mentioning that, in order to observe the difference between the semi-active laws, it is necessary to zoom in. The difference in H_2 is negligible, however for MTVV and H_∞ there are differences for higher amplitudes. As it can be obtained, the results of STMDs are low-dependent on structure model.

The reduction for each case is 70.57%, 77.22% and 78.74% (MTVV), 88.18%, 91.20% and 91.71% (H_∞) and 31.04%, 38.90% and 38.96% (H_2) for passive TMD, STMD 1 and STMD 2, respectively.

4.2 Multi-degree of freedom system

4.2.1 Nominal case

Fig. 11 shows the accelerations responses and their corresponding frequency spectra. The reduction for each case is 18.64%, 61.19% and 64.03% (MTVV), 28.28%, 69.11% and 71.01% (H_∞) and 29.73%, 51.59% and 52.81% (H_2) for passive TMD, STMD 1 and STMD 2, respectively. Both semi-active devices have a very similar performance and much better than the passive one.

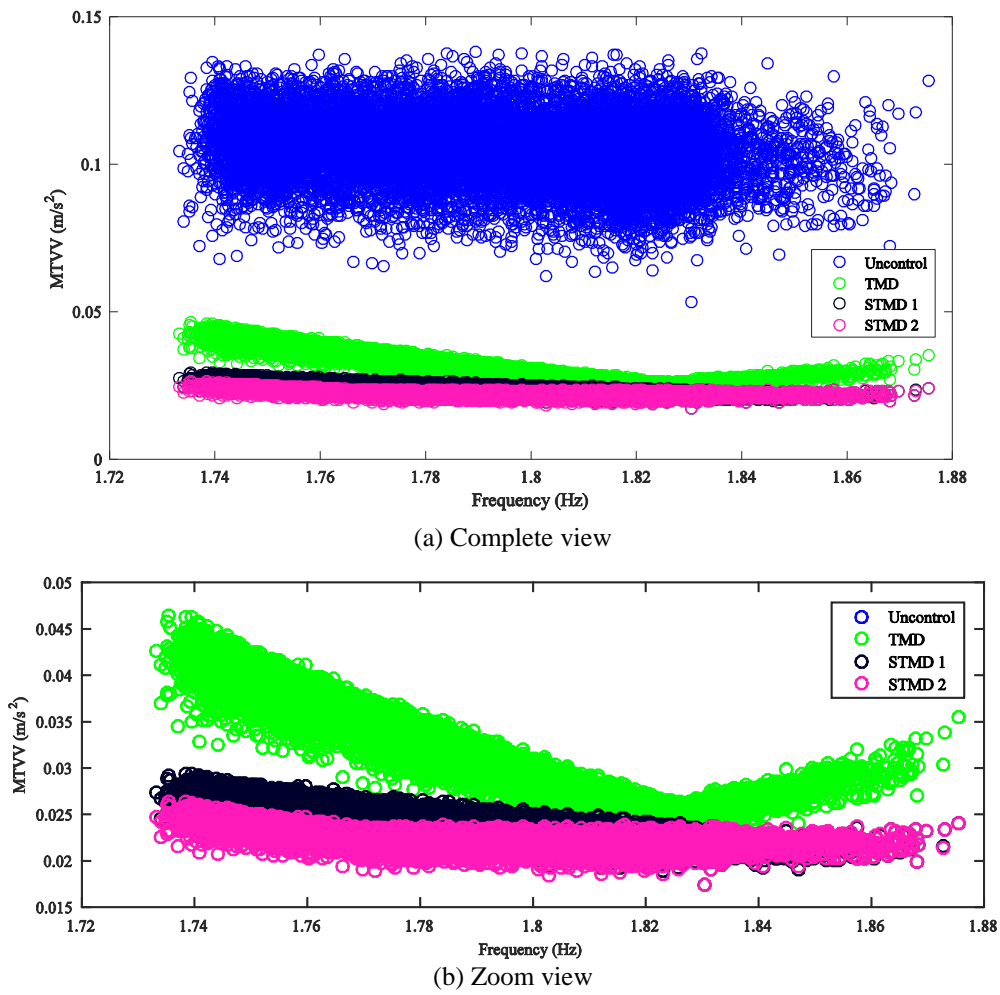


Fig. 9 MTVV vs Frequency

Table 3 Summary of results for each case

Case	Magnitude	Control	SDOF	MDOF
Nominal	MTVV reduction (%)	TMD	79.04	18.64
		STMD 1	84.08	61.19
		STMD 2	83.78	64.03
	H_∞ reduction (%)	TMD	90.23	28.28
		STMD 1	92.69	69.11
		STMD 2	92.69	71.01
H_2 reduction (%)	TMD	34.57	29.73	
	STMD 1	42.28	51.59	
	STMD 2	42.75	52.81	
Full year	MTVV reduction (%)	TMD	70.57	10.82
		STMD 1	77.22	42.85
		STMD 2	78.74	44.20
	H_∞ reduction (%)	TMD	88.18	33.85
		STMD 1	91.20	69.83
		STMD 2	91.71	70.92
H_2 reduction (%)	TMD	31.04	19.71	
	STMD 1	38.90	38.04	
	STMD 2	38.96	37.56	

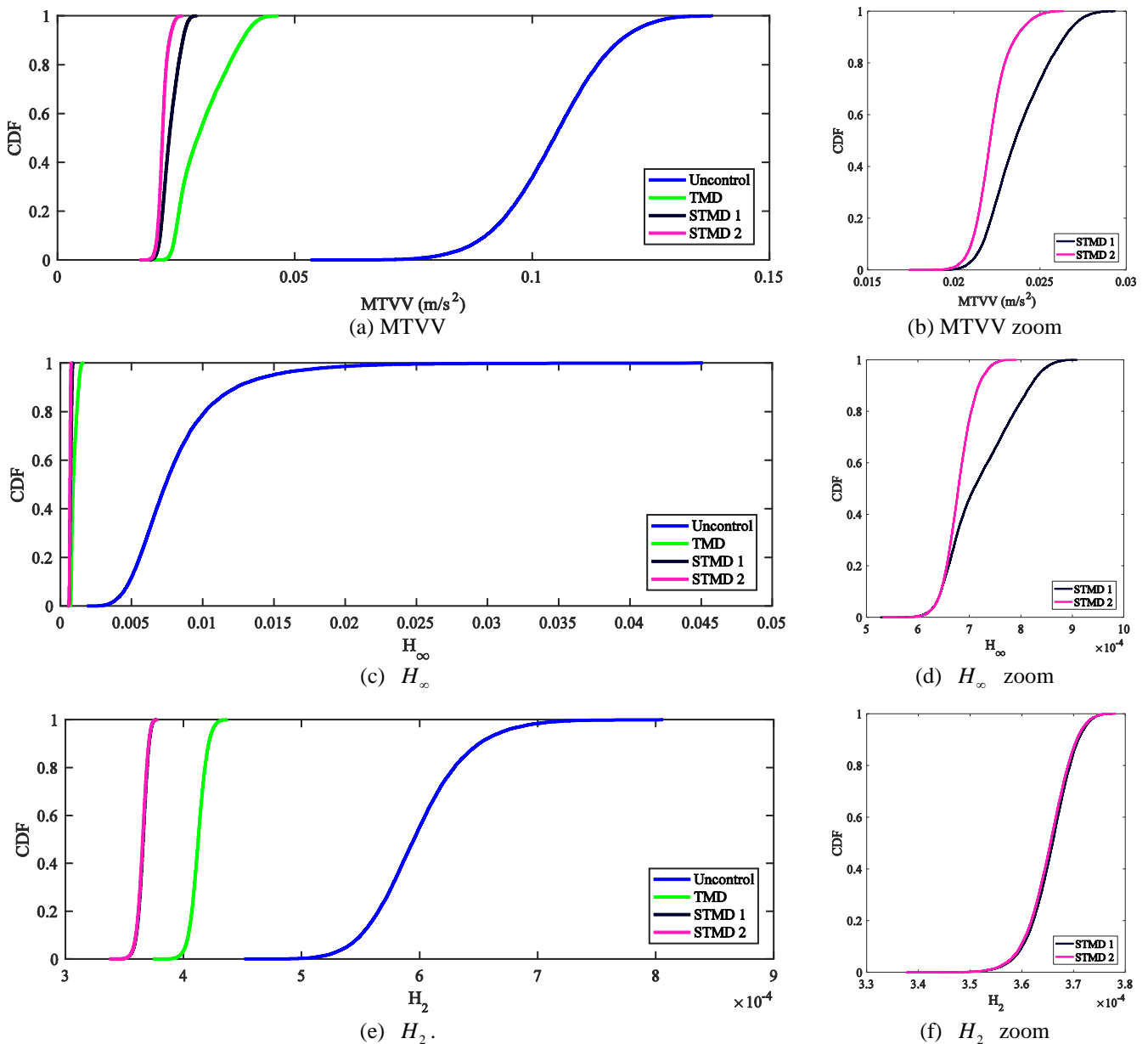


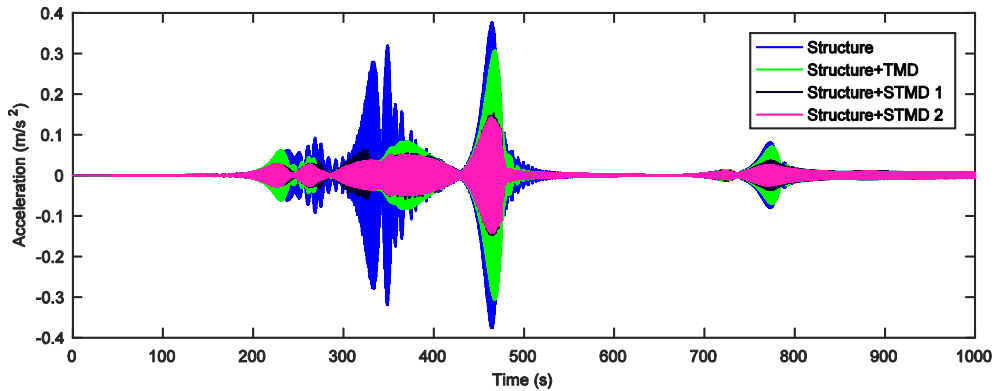
Fig. 10 CDF for SDOF case

4.2.2 Full year tests

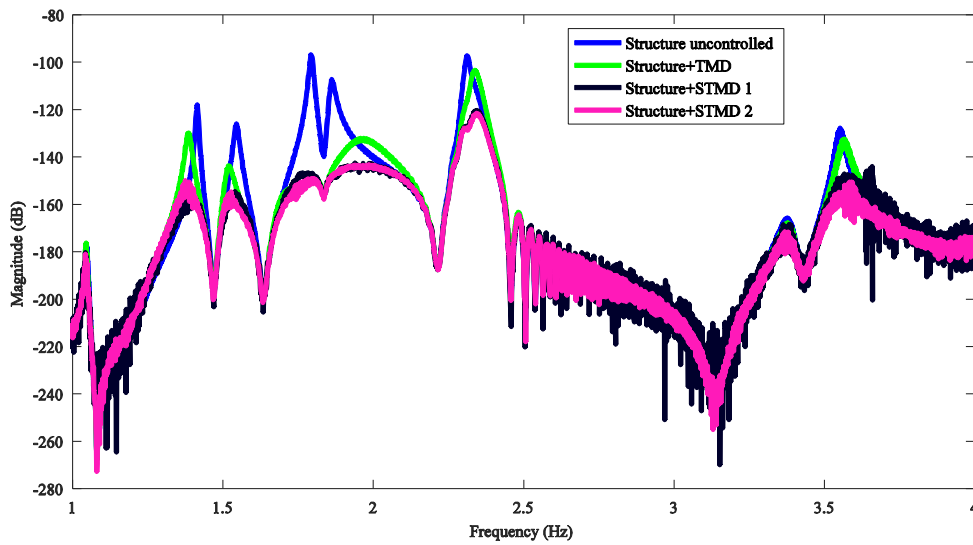
As for the SDOF system for full year tests, the TMD properties are tuned to the most repeated structural properties. Fig. 12 shows CDF curves obtained for this case. The reduction for each case is 10.82%, 42.85% and 44.20% (MTVV), 33.85%, 69.83% and 70.92% (H_2) and 19.71%, 38.04% and 37.56% (H_2) for passive TMD, STMD 1 and STMD 2, respectively. Again, both STMDs have similar performance and much better than the passive one. The inclusion of multiple modes degrades drastically the performance of control strategies. This effect is much more apparent for the TMD.

5. Conclusions

A complete study has been carried out in order to explore different practical semi-active control strategies to reduce vibration in a frequency-varying real structure over a full year monitoring taking into account only one mode or several closed-frequency modes. This study will help in making a decision about the more convenient semi-active control technique to be considered for a future implementation as well as to quantify their improvements with respect to the passive system.



(a) Time domain, time histories



(b) Frequency domain, frequency spectrum

Fig. 11 Response of MDOF system

Table 3 summarizes the results described in Section 4. Thus, the following conclusions can be drawn:

- The structure analyzed shows plenty of vibration modes with closed-space frequencies in a critical short frequency range (below 4 Hz). The modal properties of these modes change over the year mainly due to temperature variations. This fact together with the human-induced vibrations that overcome recommended serviceability limits, makes this structure an ideal candidate to implement a semi-active control strategy.
- A comprehensive study using SDOF and MDOF systems and accounting for full year tests has been carried out. A chirp function amplitude-weighted has been employed as excitation. The amplitude weighting accounts for the different loading factor depending on the excitation frequency. Several vibration reduction indexes, in frequency and time domain, have been computed in order to assess the performance of the control strategies. Interesting indexes

based on MTVV, H_∞ and H_2 norms obtained from CDFs over the year have been proposed.

- The TMD, even though it behaves quite well, degrades its performance significantly when modal frequencies of the targeted vibration mode (SDOF) move away from the nominal model. Besides, it worsens abruptly when different modes of vibration are excited (MDOF).
- Both STMDs, 1 and 2, have been shown to be quite insensitive to its initial tuning and able to cancel effectively the vibration independently of the modal properties of the tuned vibration mode (SDOF) and, also other vibration modes (MDOF) over the full year.
- There is a slightly better performance with the STMD 2 but it turns out to be insignificant for the study carried out through this paper as compared to the simplicity that STMD 1 has for practical implementation.

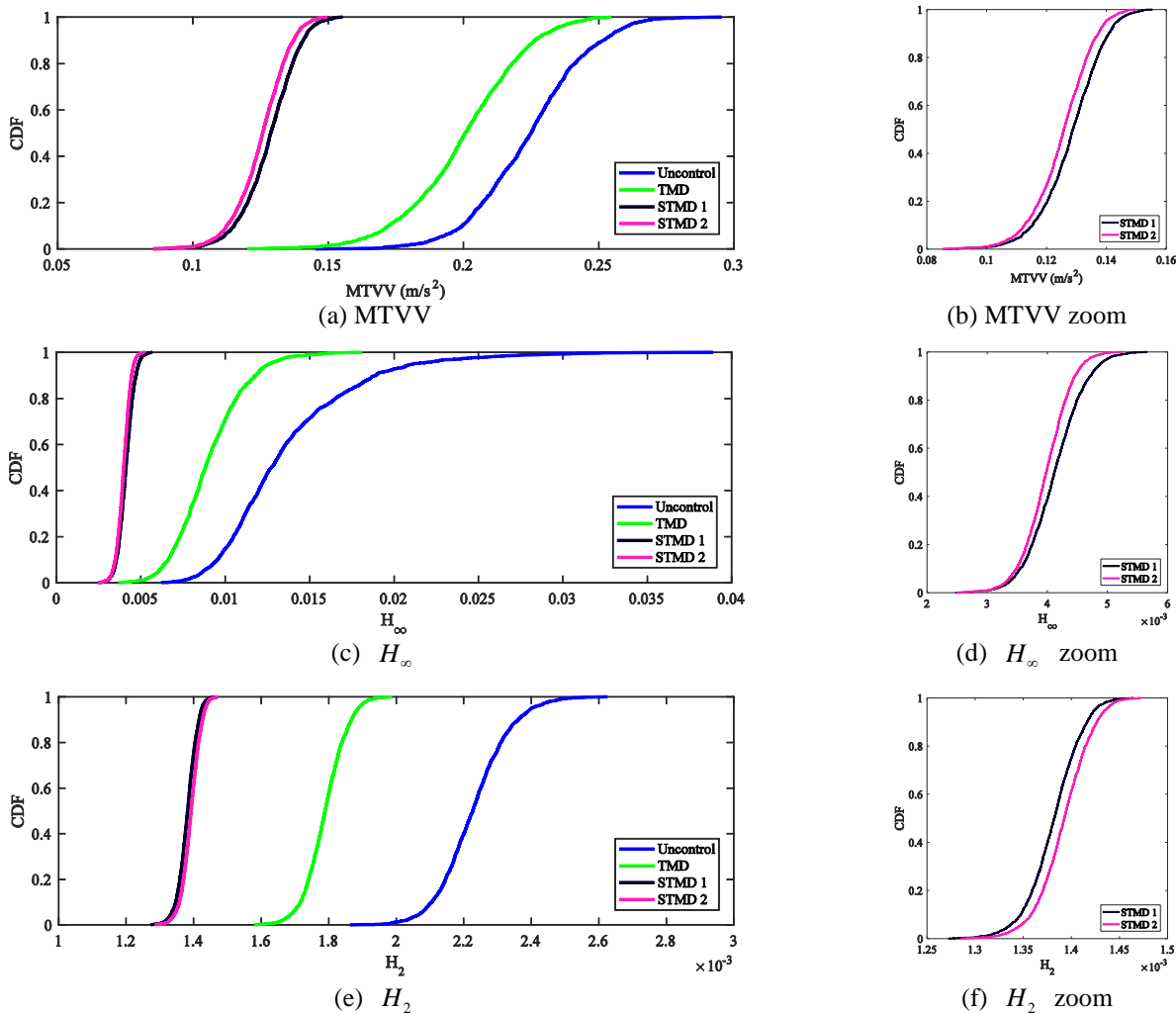


Fig. 12 CDF for MDOF case

Acknowledgments

The authors acknowledge the financial support provided by the Ministry of Economy and Competitiveness of the Government of Spain to make this work possible by funding from the REVES-P Research Project, with reference DPI2013-47441.

References

- Askari, M., Li, J. and Samali, B. (2016), "Semi-active control of smart building-MR damper systems using novel TSK-Inv and max-min algorithms", *Smart Struct. Syst.*, **18**(5), 1005-1028. doi:10.12989/sss.2016.18.5.1005.
- Bortoluzzi, D., Casciati, S., Elia, L. and Faravelli, L. (2015), "Design of a TMD solution to mitigate wind-induced local vibrations in an existing timber footbridge", *Smart Struct. Syst.*, **16**(3), 459-478. doi:10.12989/sss.2015.16.3.459.
- Brownjohn, J.M.W., Pavic, A. and Omenzetter, P. (2004), "A spectral density approach for modeling continuous vertical forces on pedestrian structures due to walking", *Can. J. Civil Eng.*
- Caetano, E., Cunha, A., Moutinho, C. and Magalhães, F. (2010), "Studies for controlling human-induced vibration of the Pedro EInês footbridge, Portugal. Part 2: Implementation of tuned mass dampers", *Eng. Struct.*, **32**(4), 1082-1091. doi:10.1016/j.engstruct.2009.12.033.
- Casado, C.M., Díaz, I.M., Sebastián, J., Poncela, A.V. and Lorenzana, A. (2013), "Implementation of passive and active vibration control on an in-service footbridge", *Struct. Control Health Monit.*, **20**, 70-87. doi:10.1002/stc.
- Casciati, F. and Casciati, S. (2016), "Designing the control law on reduced-order models of large structural systems", *Struct. Control Health Monit.*, **23**(4), 707-718. doi:10.1002/stc.1805.
- Casciati, F., Magonette, and Marazzi, F. (2006), *Technology of Semiactive Devices and Applications in Vibration Mitigation*. John Wiley & Sons Inc.
- Castaño, J., Cosido, O., Pereda, J., Cacho-Pérez, M. and Lorenzana, A. (2015), "Static, modal and dynamic behaviour of a strees ribbon footbridge: experimental and computational results", *Proceedings of the 3rd International Conference on Mechanical Models in Structural Engineering (CMMoST 2015)*.
- Chang, C.M., Wang, Z., Spencer Jr., B.F. and Chen, Z. (2013), "Semi-active damped outriggers for seismic protection of high-rise buildings", *Smart Struct. Syst.*, **11**(5), 435-451. doi:10.12989/sss.2013.11.5.435.
- Chung, L.L., Lai, Y.A. and Yang, C.S.W. (2013), "Semi-active

- tuned mass dampers with phase control”, *J. Sound Vib.*, **332** (15), 1-16. doi:10.1016/j.jsv.2013.02.008.
- Den Hartog, J.P. (1985), *Mechanical Vibrations*. Courier Co.
- Gunaydin, M., Adanur, S., Altunisik, A.C. and Sevim, B. (2015), “Static and dynamic responses of halgavor footbridge using steel and FRP materials”, *Steel Compos. Struct.*, **18**(1), 51-69. doi:10.12989/scs.2015.18.1.051.
- Jung, H.J.J., Spencer Jr., B.F., Ni, Y.Q., Lee, I.W. (2004), “State-of-the-art of semiactive control systems using MR fluid dampers in civil engineering applications”, *Struct. Eng. Mech.*, **17**(3-4), 493-526. doi:10.12989/sem.2004.17.3_4.493.
- Koo, J.H., Ahmadian, M. Setareh, M. and Murray, T. (2004), “In search of suitable control methods for semi-active tuned vibration absorbers”, *J. Vib. Control*, **10**(2), 163-174. doi:10.1177/1077546304032020.
- Moutinho, C. (2015), “Testing a simple control law to reduce broadband frequency harmonic vibrations using semi-active tuned mass dampers”, *Smart Mater. Struct.*, **24**(5). IOP Publishing: 55007. doi:10.1088/0964-1726/24/5/055007.
- Moutinho, C., Cunha, A. and Caetano, E. (2010), “Analysis and control of vibrations in a stress-ribbon footbridge”, *Struct. Control Health Monit.*, doi:10.1002/stc.
- Moutinho, C., Magalhães, F. and Caetano, E. (2015), “Analysis of the vibration levels of a slender footbridge measured by continuous dynamic monitoring system”, *In COMPDYN 2015*. Crete Island, Greece.
- Nagarajaiah, S. and Jung, H.J. (2014), “Smart tuned mass dampers: Recent developments”, *Smart Struct. Syst.*, **13** (2), 173176.
- Narros, A J. (2011), “Pasarela Peatonal ``Pedro Gómez Bosque`` Sobre El Río Pisuerga En La Ciudad de Valladolid. Un Nuevo Récord de Longitud En Pasarelas Colgadas de Banda Tesa”, *Revista Técnica Cemento-Hormigón*, **947**, 80-86 (in spanish).
- Peeters, Bart, and Guido De Roeck. (1999), “Reference-based stochastic subspace identification for output-only modal analysis”, *Mech. Syst. Signal Pr.*, **13**(6), 855-878. doi:10.1006/mssp.1999.1249.
- Pereira, E., Díaz, I.M., Hudson, E.J. and Reynolds, P. (2014), “Optimal control-based methodology for active vibration control of pedestrian structures”, *Eng. Struct.*, **80**, 153-162. doi:10.1016/j.engstruct.2014.08.046.
- Sebastián, J.de, Escudero, A., Arnaz, R., Díaz, I.M., Poncela, A. and Lorenzana, A. (2013), “A low-cost vibration monitoring system for a stress-ribbon footbridge”, *Proceedings of the 6th ECCOMAS Conference on Smart Structures and Materials*.
- Soria, J.M., Díaz, I.M., García-Palacios, J.H. and Ibán, N. (2016), “Vibration monitoring of a steel-plated stress-ribbon footbridge: uncertainties in the modal estimation”, *J. Bridge Eng.*, **21**(8), 1-13. doi:10.1061/(ASCE)BE.1943-5592.0000830.
- Standard, I.S.O. (2007), “ISO 10137: Bases for Design of structure—Serviceability of Buildings and Walkways against Vibrations”, *Geneva: ISO*.
- Wang, X., Díaz, I.M. and Pereira, E. (2016), “MIMO control design including input-output frequency weighting for human-induced vibrations”, *Proceedings of the EACS 2016 -- 6th European Conference on Structural Control*. Sheffield, U.K.
- Weber, F. (2013), “Dynamic characteristics of controlled MR-STMDs of wolgograd bridge”, *Smart Mater. Struct.*, **22**(9): 95008. doi:10.1088/0964-1726/22/9/095008.
- Weber, F., Feltrin, G. and Huth, O. (2006), “Guidelines for structural control”, *SAMCO Final Report*. Dubendorf, Switzerland.